Bioprocess Engineering 7 (1992) 335–341

Bioprocess Engineering

A kinetic model and simulation of starch saccharification and simultaneous ethanol fermentation by amyloglucosidase and Zymomonas mobilis

C.-G. Lee, C. H. Kim and **S. K. Rhee,** Taejon, Korea

Abstract. A mathematical model is described for the simultaneous saccharification and ethanol fermentation (SSF) of sago starch using amyloglucosidase (AMG) and Zymomonas mobilis. By introducing the degree of polymerization (DP) of oligosaccharides produced from sago starch treated with α-amylase, a series of Michaelis-Menten equations were obtained. After determining kinetic parameters from the results of simple experiments carried out at various substrate and enzyme concentrations and from the subsite mapping theory, this model was adapted to simulate the SSF process. The results of simulation for SSF are in good agreement with experimental results.

List of symbols

α	g/g	rate coefficient of production
μ_{max}	1/h	maximum specific growth rate
E	%, v/w	AMG concentration
G_1	mmol/l	glucose concentration
G_c	mmol/l	glucose concentration consumed
G_f	mmol/l	glucose concentration formed
G_n	mmol/l	n-mer maltooligosaccharide concentration
K_i	g/l	ethanol inhibition constant for ethanol production
K_g	mmol/l	glucose inhibition constant for glucose production
K_p	mmol/l	glucose limitation constant for ethanol production
K_x	mmol/l	glucose limitation constant for cell growth
$K_{m,n}$	mmol/l	Michaelis-Menten constant for n-mer oligosaccharide
k_e	%, v/w	enzyme limitation constant
k_{es}		proportional constant
$k_{max,n}$	1/s	maximal velocity for n-mer digestion
k_s	g/l	substrate limitation constant
m_s	g/g	maintenance energy
MW_n	g/mol	molecular weight of n-mer oligosaccharide
P	g/l	ethanol concentration
P_0	g/l	initial ethanol concentration
P_m	g/l	maximal ethanol concentration
Q_{pm}	g/(g · h)	maximum specific ethanol production rate
S_n	mmol/h	branched n-mer oligosaccharide concentration
S_0	g/l	initial starch concentration
S_{sta}	g/l	starch concentration
S_{tot}	g/l	total sugar concentration
$V_{max,n}$	1/h	maximum digestion rate of n-mer oligosaccharide
V_0	g/(l · h)	initial glucose formation rate
X	g/l	cell mass
X_0	g/l	initial cell mass
$Y_{p/s}$	g/g	ethanol yield
$Y_{x/s}$	g/g	cell mass yield

1 Introduction

For industrial ethanol fermentation, starch is being used as a main substrate due to its global abundance and comparatively low price [1–3]. In order to be utilized by ethanologenic microorganisms such as yeasts or a bacterium Zymomonas mobilis, however, starch must be hydrolyzed into glucose units prior to alcohol fermentation. This can be achieved by use of two enzymes, namely, α-amylase and amyloglucosidase (AMG). The former reacts endogenously with α-(1→4) glucosidic linkages of polysaccharides to produce oligosaccharides and the latter hydrolyzes exogenously the nonreducing end α-(1→4), α-(1→6) and α-(1→3) glucosidic linkages of oligosaccharides to produce glucose [4]. The reaction rate of each enzyme depends on the chain length of the oligosaccharides [5].

The conventional ethanol fermentation processes using liquefied starch as substrate comprise two separate operations which have significant consequences viz. costs; the presaccharification of starch and ethanol fermentation. In contrast, the simultaneous saccharification and fermentation (SSF) process combines these two steps into one to offer the potential of an increased rate of hydrolysis. In this cost-effective alternative process, the product inhibition on saccharification by glucose can be diminished since the glucose produced from oligosaccharides is consumed immediately by the cells and converted into ethanol [1].

Although considerable attention has been paid to SSF itself, there are few studies reporting practical kinetic models for SSF process [6–8]. Especially for glucose production by exo-cleavage of starch, no adaptable models have been reported. Concentrated on this fact, attempts were made to propose a reliable kinetic model for this single step process, which can be used to develop or optimize SSF processes using Z. mobilis cells and sago starch as substrate.

2 Model system

2.1 Assumptions for kinetic studies

(1.) After liquefaction by α-amylase, oligosaccharides with the degree of polymerization (DP) below 7 are main products of α-amylase from Bacillus licheniformis [5]. Among them, only residual maltose, maltotriose and maltopentaose are major products of liquefaction. Consequently, the α-(1→6) and α-(1→3) terminal bonds are taken into consideration only in the oligosaccharides of DP 2, DP 3 and DP 5. (2.) The rates of hydrolysis of α-(1→6) and α-(1→3) bonds by AMG are approximately one-twentieth of the rate of corresponding α-(1→4) bond [9]. (3.) Kinetic parameters, Michaelis-Menten constant (K_m) and molecular activity (k_{max}) for the hydrolysis of oligosaccharides (from DP 2 to DP 7) were determined by the subsite mapping theory [10–12]. (4.) There is no change in enzymatic activity during fermentation period [1, 13]. Thus, the enzyme affinities to each oligosaccharide are irrelevant to enzyme and substrate concentrations.

2.2 Models for glucose production by AMG

According to the subsite mapping theory, AMG has 7 subsites which can produce enzyme-oligosaccharide complexes and their affinities to oligosaccharides are closely related to the chain length of oligosaccharides [14–18]. Thus, in AMG-catalyzed saccharification of oligosaccharides, the increase in the degree of polymerization of substrates results in the increase of reaction velocity (V) and concomitant decrease of Michaelis-Menten constant (K_m) [11, 12]. Based on the assumptions made previously, the reaction rate of releasing free glucose units from oligosaccharides can be expresed by a series of Michaelis-Menten equations as follows:

$$\frac{dG_n^*}{dt} = -\frac{V_{max,n} \cdot G_n}{K_{m,n}+G_n} \cdot \frac{K_g}{K_g+G_1} \qquad (n=2 \text{ to } 7), \tag{1}$$

$$\frac{dS_n}{dt} = -\frac{(V_{max,n}/20)\, S_n}{K_{m,n}+S_n} \cdot \frac{K_g}{K_g+G_1} \qquad (n=2, 3, 5), \tag{2}$$

$$\frac{dG_n}{dt} = \frac{dG_n^*}{dt} - \frac{dG_{n+1}^*}{dt} \qquad (n=3, 5, 6), \tag{3}$$

$$\frac{dG_n}{dt} = \frac{dG_n^*}{dt} - \frac{dG_{n+1}^*}{dt} + \frac{dS_{n+1}}{dt} \qquad (n=2, \text{ and } 4), \tag{4}$$

$$\frac{dG_f}{dt} = -\left(\sum_{n=3}^{7} \frac{dG_n}{dt}\right) - 2\left(\frac{dG_2}{dt} + \frac{dS_2}{dt}\right), \tag{5}$$

where G_n is the molar concentration of n-mer maltooligosaccharides, dG_n^*/dt is the pure cleavage rate of those n-mer oligosaccharides, dG_n/dt is the net change rate including the formation rate from (n+1)-mer digestion and S_n is the molar concentration of α-(1→6) and α-(1→3) branched n-mer oligosaccharides. The schematic diagram of this reaction series is shown in Fig. 1. Thus, the resulting Eq. (5) represents the total formation rate of glucose without any consumption. $K_{m,n}$ and $V_{max,n}$ are Michaelis-Menten constants and the maximum cleavage velocities for given n-mer substrates, respectively.

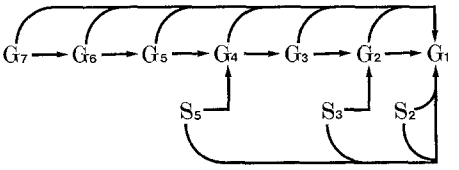

Fig. 1. The schematic diagram for glucose production by AMG. G_n and S_n denote linear and branched n-mer oligosaccharides, respectively

Table 1. Theoretically obtained parameters for AMG-catalyzed hydrolysis of oligosaccharides

Substrate	*DP (n)*	$K_{m,n}$ ($\times 10^3$, M)	$k_{max,n}$ (1/s)
Maltose	2	1.20	3.01
Maltotriose	3	0.402	9.97
Maltotetraose	4	0.273	16.7
Maltopentaose	5	0.204	21.1
Maltohexaose	6	0.100	16.0
Maltoheptaose	7	0.121	20.3

Table 1 represents the parameters obtained by the subsite mapping theory for the above equations. The V_{max} values, however, must be calibrated from the maximum molecular activity, K_{max}, by considering both enzyme and initial substrate concentrations before introducing the above model equations. From the assumption (4), this correction can be made by the fact that the initial glucose formation rate, V_0, must equal to the sum of all components as in Eqs. (6) and (7):

$$V_0(E, S_0) = \sum_{n=1}^{7} V_{max,n}(E, S_0), \tag{6}$$

$$V_{max,n}(E, S_0) = k_{max,n} \cdot k_{es} \cdot \frac{E}{E+k_e} \cdot \frac{S_0}{S_0+k_s}, \tag{7}$$

where E and S_0 are AMG and the initial starch concentrations in the fermentation broth, respectively, and k_{es}, k_e and k_s are constants. In this summation, the portions attributed from α-(1→6) and α-(1→3) branched n-mer oligosaccharides can be neglected by using the assumption (2).

Simultaneous integration of Eqs. (1) through (5) by the fourth order Runge-Kutta-Gill method [19] gives the glucose (G_1) profile. Total sugar concentration (S_{tot}) and starch (oligosaccharides) concentration (S_{sta}) are expressed as in equations (8) and (9), respectively:

$$S_{tot} = \sum_{n=1}^{7} (G_n \cdot MW_n) + \sum_{n=2,3,5} (S_n \cdot MW_n), \tag{8}$$

$$S_{sta} = S_{tot} - G_1 \cdot MW_1, \tag{9}$$

$$MW_n = 180\, n - 18\,(n-1), \tag{10}$$

where MW_n is the molecular weight of the n-mer oligosaccharide.

2.3 Models for other fermentation variables

For cell growth, the following model is used by modifying the growth kinetic models proposed by Levenspiel [20], Ghose et al. [21] and Bazua and Wilke [22] which take the dependence of cell growth on the concentration of glucose and ethanol present in the fermentation broth into account:

$$\frac{dX}{dt} = \mu_{max}\left[\frac{G_1}{G_1+K_x}\right]\left[1-\frac{P}{P_m}\right]X . \tag{11}$$

where P_m is the maximal ethanol concentration for cell growth and can be determined easily by a simple experiment. The substrate inhibition by the high concentration of glucose has been neglected in this model equation since glucose does not accumulate in SSF process.

For ethanol production, a modified partially growth-associated Ludeking-Piret model [23] is introduced by taking the ethanol inhibition and glucose limitation terms into account:

$$\frac{dP}{dt} = Q_{pm}\left[\frac{G_1}{G_1+K_p}\right]\left[\frac{K_i}{K_i+P}\right]X+\alpha\frac{dX}{dt} \tag{12}$$

The rate of glucose consumption can be calculated by using product yield coefficient ($Y_{p/s}$) calculated from the basis of total substrate consumed as follows:

$$\frac{dG_c}{dt} = -\frac{1}{MW_1}\cdot\frac{dP}{dt}\cdot\frac{1}{Y_{p/s}} \tag{13}$$

Finally, the rate equation for glucose accumulation in the fermentation broth can be obtained by the summation of Eqs. (5) and (13):

$$\frac{dG_1}{dt} = \frac{dG_f}{dt}+\frac{dG_c}{dt} \tag{14}$$

Simultaneous numerical integration of Eqs. (11), (12) and (14) gives the most important fermentation variables such as cell mass, ethanol and glucose concentrations. Eqs. (8) and (9) also can be used to calculate starch and total sugar concentrations during the fermentation processes.

3 Materials and methods

3.1 Strains and media

The strain used for this study was Z. mobilis ZM4 (ATCC 31821). It was maintained and grown in a liquid medium containing 100 g/l glucose, 10 g/l yeast extract, 1 g/l KH_2PO_4, 1 g/l $(NH_4)_2SO_4$ and 0.5 g/l $MgSO_4 \cdot 7H_2O$ [24]. This medium was also used to prepare an inoculum. For fermentation, sago starch which is a product extracted from the seed or tuberous stems of palms and cycads such as Metroxylon sagu and a mixture of 27% (w/w) amylose and 73% (w/w) amylopectin [25] was used as substrate. This starch has been assessed as substrate for ethanol production and proven to be an effective substitute for glucose [26]. The total sugar concentration estimated by measuring the dextrose equivalent (DE) produced by hydrolysis with 1 N HCl for 2 h at 100 °C, was 0.93 g/g of sago starch. The fermentation medium consisted of 50–250 g sago starch and 10 g yeast extract (Difco, USA) per liter of tap water and was sterilized by autoclaving for 15 min at 121 °C after α-amylase treatment.

3.2 Enzymes used for liquefaction and saccharification of starch

Two enzymes, thermostable α-amylase (Thermamyl-60) of Bacillus licheniformis origin, and amyloglucosidase (AMG 200 l) from Aspergillus niger, were employed. The enzymatic activites of these enzymes were 60 KNU/g and 200 AGU/ml, respectively, as defined by Novo Industri [27]. 1 KNU is defined as the amount of enzyme that can hydrolyze 5.26 g soluble starch per hour at pH 5.6 and 37 °C and 1 AGU is the amount of enzyme which cleaves 1 μmole of maltose per min at pH 4.3 and 25 °C.

3.3 Experimental conditions

A slurry of sago starch powder in tap water (50–250 g/l) was adjusted to pH 6.5 by the addition of 1 N NaOH. Liquefaction of starch was carried out by adding 0.2% (v/w) Termamyl to the slurry and incubating at 95 °C for 1 h. A 250 ml flask was used as the reactor for the starch digestion experiment to calculate the initial glucose formation rate. The flask containing desired amount of initial starch was incubated at pH 5.0 and 35 °C in a shaking water bath after proper amount of AMG was loaded. At regular intervals, 1 ml of sample was collected to measure the glucose concentration. SSF was carried out in a 2 l fermentor (New Brunswick Chemostat, Model C-32) under non-aerated conditions at desired temperatures with mild agitation. The initial pH was adjusted to 5.0 using 1 N HCl. Inocula (50 ml) were grown in 250 ml flasks at 35 °C for 20 hours and added to the fermentation medium (1 l). The AMG dosage was 0.2–1.0% (v/w).

3.4 Analytical methods

Ethanol, dry cell weight, total sugar and reducing sugar were determined as described previously [26]. Glucose was determined by the glucose oxidase/peroxidase method using Sigma diagnostic kits (Glucose No. 510).

4 Results and discussion

Measurements of initial reaction rate for the calculation of parameters corresponding to initial glucose formation rate

(V_0) were carried out at various AMG and starch concentrations at pH 5.0 and 35 °C. Typical trends of V_0 with various concentrations of AMG loaded and initial starch concentrations are shown in Fig. 2. From the experimental data, three constants (k_{es}, k_e and k_s) in Eq. (7) were evaluated to obtain V_0 as a function of AMG concentration (E) and initial starch concentration (S_0). The resulting values are listed in Table 2. By use of these values as correction factors, V_{max} values for each substrate concentration were calculated at various concentrations of AMG and S_0 from Eqs. (6) and (7).

Simultaneous numerical integration of Eqs. (1) through (5) using the values derived from Eq. (7) and initial concentrations of each oligosaccharide at initial starch concentration of 150 g/l and enzyme concentration of 1.0% (v/w) enabled us to predict the actual concentrations of glucose and other oligosaccharides with DP 2 to DP 7 excellently. The initial values used in the numerical integration are shown in Table 3. The comparison of calculated and experimental profiles of glucose together with the estimated concentrations of oligosaccharides is demonstrated in Fig. 3. From these results, it can be seen that the hydrolysis of oligosaccharides with DP 2, DP 3 and DP 5 in which there are α-(1→6) and/or α-(1→3) linkages besides α-(1→4) is slower than that of the others which contain only α-(1→4) linkages. The reaction rate differences between these oligosaccharides are due to the fact that AMG has higher affinity for longer chains [14].

Comparisons of the model predictions for the glucose production with experimental data were made at various concentrations of initial starch and/or AMG. As can be seen in Fig. 4, the rate of saccharification in the model predictions

Table 2. Values of constants used in the model equations

Constant	Value	Reference
k_{es}	0.369	calculated
k_e	0.462% (v/w)	calculated
k_s	32.4 g/l	calculated
$Y_{p/s}$	0.487 g/g	experimental
$Y_{x/s}$	0.0146 g/g	experimental
P_0	3.0 g/l	experimental
P_m	90.0 g/l	experimental
Q_{pm}	5.1 g/g/h	experimental
X_0	0.18 g/l	experimental
μ_{max}	0.303 1/h	experimental
α	11.0 g/g	simulated
K_g	1.0 mmol/l	simulated
K_i	55.0 g/l	simulated
K_p	7.0 mmol/l	simulated
K_x	2.0 mmol/l	simulated
m_s	0.02 g/g	simulated

Table 3. Initial values used in numerical integrations

DP (n)	G_n/S_0 (fraction)	(S_n/S_0) (fraction)	$V_{max\,n}$ ($\times 10^{-4}$, 1/h)
1	0.0077	–	–
2	0.0734	0.0313	1.0836
3	0.1328	0.0432	3.5892
4	0.0975	–	6.0120
5	0.2244	0.0493	7.5960
6	0.2683	–	5.7600
7	0.0723	–	7.3080

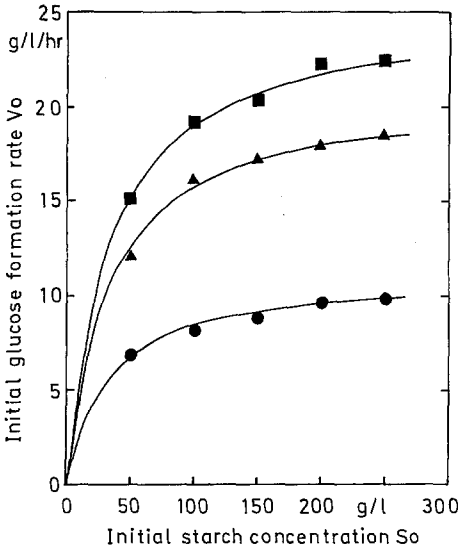

Fig. 2. Effect of AMG concentration E on initial saccharification rate of starch. Lines represent predicted values and symbols experimental values. (●) 0.2%; (▲) 0.6%; (■) 1.0%

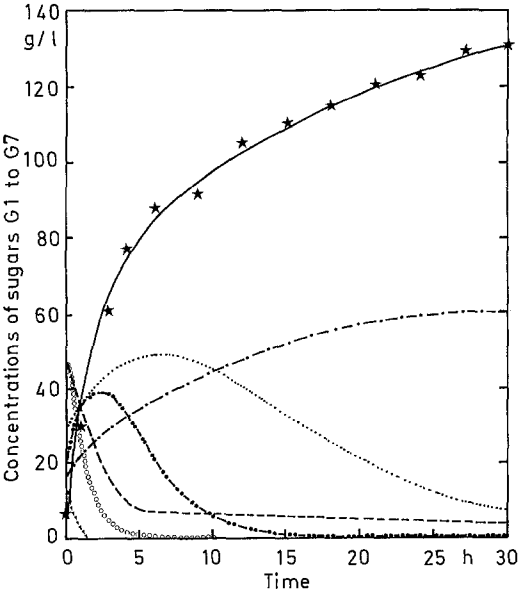

Fig. 3. Calculated profiles (lines) of glucose and other oligosaccharides with DP 2 to DP 7 compared with experimental glucose concentration (★). (——) G_1; (– · –) G_2; (· · ·) G_3; (– · · –) G_4; (– – –) G_5; (ooo) G_6; (►►►) G_7

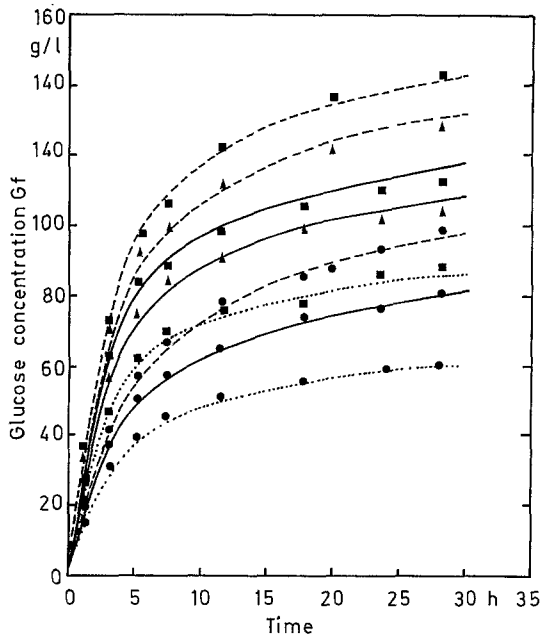

Fig.4. Profiles of pedicted (lines) and experimental (symbols) glucose concentration G_f at various initial starch and AMG concentrations, S_0 and E. Initial starch concentration S_0: (· · ·) 100 g/l; (——) 150 g/l; (– – –) 200 g/l. AMG concentration E: (●) 0.2%; (▲) 0.6%; (■) 1.0%

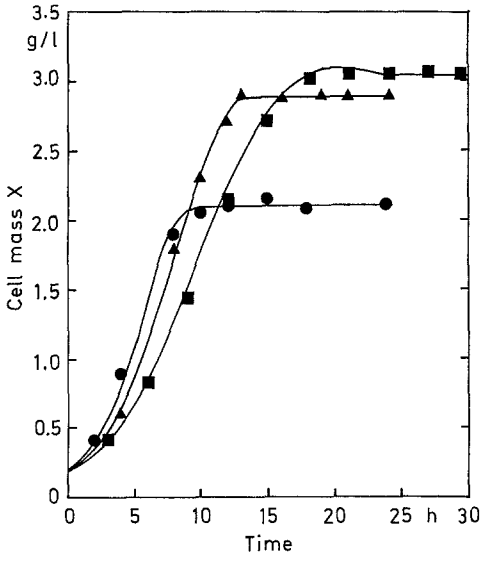

Fig. 5. Effect of initial starch concentration S_0 on growth (X) of Zymomonas mobilis. Comparison of calculated curves (lines) from Eq. (11) with experimental data (symbols). S_0: (●) 100 g/l; (▲) 150 g/l; (■) 200 g/l

also fits well with experimental data. It was clear that the increased initial starch and/or AMG concentrations resulted in an increased initial rate of saccharification over the ranges tested.

SSF was undertaken with various initial sago starch and AMG concentrations at pH 5.0 and 35 °C. In most modelling studies for Z. mobilis ethanol inhibition kinetics are of a linear type with a threshold ethanol concentrations [28–31]. For the adaptation of models in the fermentation process, the threshold ethanol concentrations for cell growth (P_m) are to be measured and taken into consideration in the model equations. In this study, the value of P_m was 90 g/l. The cell mass profiles could be obtained easily from the integration of Eq. (11). Fig. 5 shows the resulting growth curves of simulation compared with the measured data points of dry cell weight with an inoculum amount of 0.18 g/l and the AMG concentration of 1.0% (w/v). The difference in the initial growth rates at different starch concentration seems to be affected by glucose. At higher initial concentration of starch, higher glucose concentration will be generated so as to inhibit cell growth. A slight decay of cell mass in a stationary phase at the initial starch concentration of 200 g/l is due to cell death caused by high ethanol concentration in the fermentation broth.

To obtain ethanol and glucose concentration profiles in SSF system, parameters in Eq. (12) were determined first. Because the fermentation variables, e.g. X, P and G, are mutually related to each other, iteration of simultaneous numerical integration of Eqs. (11), (12) and (14) was performed to estimate the parameters of K_p, K_i, K_x and α. This iteration was done until the mean square errors converged to a minimum value using the fourth order Runge-Kutta-Gill method. Other constants such as $Y_{p/s}$ and Q_{pm} were calculated from the experimental data. Table 2 lists the values of these constants. Figs. 6 and 7 show the calculated profiles of progress curves of ethanol and glucose concentrations in SSF process.

To test the validity of this model system, simulation of whole SSF system was performed at various concentrations of AMG and initial starch. The results predicted were in good agreement with the experimental values. Fig. 8 shows the comparison of calculated profiles of cell growth, ethanol and glucose concentrations with experimental data at 200 g/l of initial starch concentration with 1.0% (v/w) AMG. The predicted values of ethanol are slightly higher than experimental data during exponential phase. For glucose, this system seems to fail to follow up the rapid increase of glucose concentration observed in the early stage of SSF. This phenomenon is probably due to the over-estimation of ethanol concentration in the early stage. As the predicted profile of glucose in the later stage is close to experimental ones, however, this over-estimation in the early production phase is not so significant in this system to develop and optimize SSF process.

In conclusion, a mathematical model should be able to estimate the variations of important fermentation variables such as glucose, starch, total sugar, ethanol and cell mass. The kinetic model proposed in this study could clearly simulate the experimental data of cell growth, glucose concentration, and production of ethanol in SSF process. However, simulations would also be needed to check directly whether suboptimal conditions exist in any operation or not, albeit

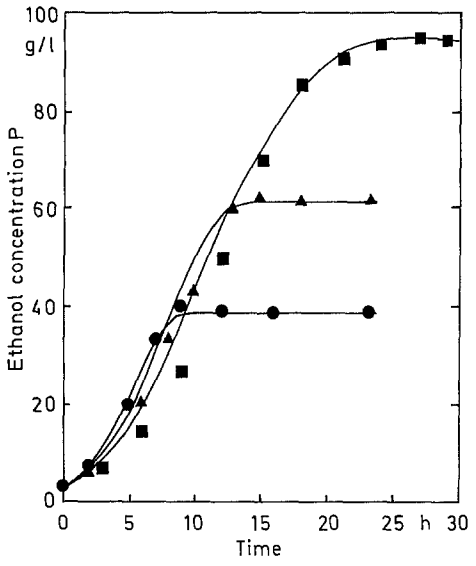

Fig. 6. Effect of initial starch concentration S_0 on simulated (lines) and experimental (symbols) ethanol production P_0. S_0: (●) 100 g/l; (▲) 150 g/l; (■) 200 g/l

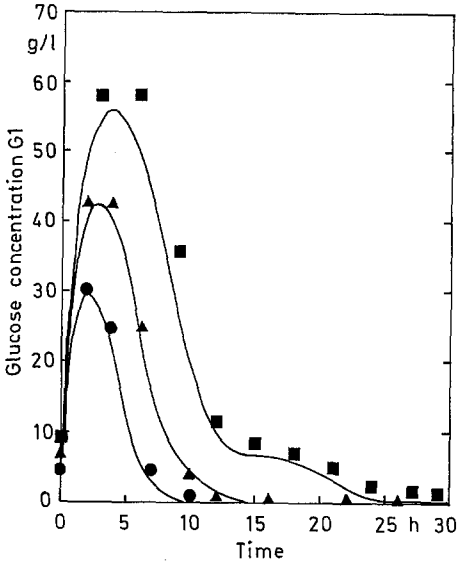

Fig. 7. Effect of initial starch concentration S_0 on simulated (lines) and experimental (symbols) glucose concentration G_1. S_0: (●) 100 g/l; (▲) 150 g/l; (■) 200 g/l

this preexamination does not always fit directly in the determination of optimal conditions for the process as a whole. Consequently, the model equations should be assessed in the other systems, e.g. semi-batch SSF with cell recycle or continuous SSF with immobilized biocatalysts to verify a generality of the proposed model for its further application.

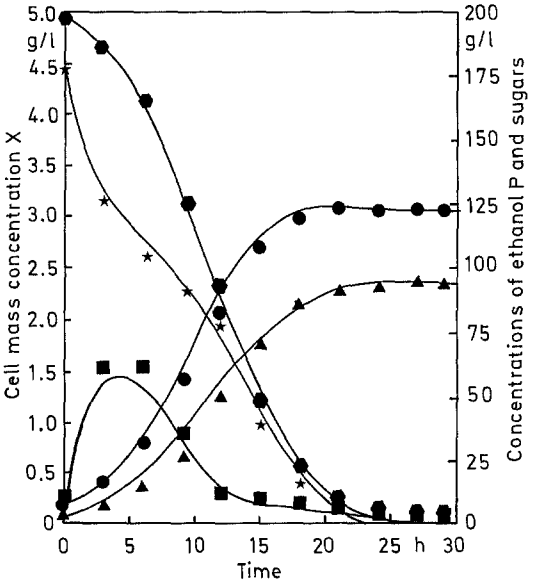

Fig. 8. Comparison of fermentation variables between predicted (lines) and experimental (symbols) SSF process. (▲) ethanol; (●) cell mass; (■) glucose; (●) total sugar; (★)

References

1. Lee, J. H.; Pagan, R. J.; Rogers, P. L.: Continuous simultaneous saccharification and fermentation of starch using Zymomonas mobilis. Biotechnol. Bioeng. 25 (1983) 659–669
2. de Menezes, T. J. B.: Starchy materials for alcohol fuel production. Process Biochem. 17 (1982) 32–35
3. Poosaran, N.; Heyes, R. H.; Rogers, P. L.: Ethanol production from cassava starch using a highly productive strain of Zymomonas mobilis and Saccharomyces uvarum ATCC 26602. Biomass. 7 (1985) 171–183
4. Pazur, J. H.; Ando, T.: The hydrolysis of glucosyl oligosaccharides with α-D-(1→4) and α-D-(1→6) bonds by fungal amyloglucosidase. J. Biol. Chem. 235 (1960) 297–302
5. Norman, B. E.: The application of polysaccharide degrading enzymes in the starch industry. In: Berkeley, R. C. W.; Gooday, G. W.; Ellwood, D. C. (Eds.): Microbial Polysaccharides and Polysaccharases, pp. 339–376. New York: Academic Press 1979
6. Ghosh, P.; Pamment, N. B.; Martin, W. R. B.: Simultaneous saccharification and fermentation of cellulose: Effect of β-D-glucosidase activity and ethanol inhibition of cellulases. Enzyme Microb. Technol. 4 (1982) 425–430
7. Asenjo, J. A.: Modelling the bioconversion of cellulose into microbial products: Rate limitations. Process Biochem. 19 (1984) 217–224
8. Lee, G. M.; Kim, C. H.; Zainal, A.; Han, M. H.; Rhee, S. K.: Sago starch saccharification and simultaneous ethanol fermentation by amyloglucosidase and Zymomonas mobilis. J. Chem. Tech. Biotechnol. 38 (1987) 235–242
9. Pazur, J. H.; Kleppe, K.: The hydrolysis of α-D-glucosides by amyloglucosidase from Aspergillus niger. J. Biol. Chem. 237 (1984) 1002–1006
10. Hiromi, K.: Interpretation of dependency of rate parameters on the degree of polymerization of substrate in enzyme-catalyzed reactions: Evaluation of subsite affinities of exo-enzyme. Biochem. Biophys. Res. Commun. 40 (1970) 1–6
11. Hiromi, K.; Nitta, Y.; Numata, C.; Ono, S.: Subsite affinities of glucoamylase: Examination of the validity of the subsite theory. Biochim. Biophys. Acta 302 (1973) 362–375
12. Tanaka, A.; Fukuchi, Y.; Ohnishi, M.; Hiromi, K.; Aibara, S.; Morita, Y.: Fractionation of isozymes and determination of the subsite structure of glucoamylase from Rhizopus niveus. Agr. Biol. Chem. 47 (1983) 573–580
13. Kim, C. H.; Lee, G. M.; Zainal, A.; Han, M. H.; Rhee, S. K.: Immobilization of Zymomonas mobilis and amyloglucosidase

for ethanol production from sago starch. Enzyme Microb. Technol. 10 (1988) 426–430
14. Ono, S.; Hiromi, K.; Zinbo, M.: Kinetic studies on gluc-amylase. I. The influence of chain length of linear substrates on the rate parameters. J. Biochem. 55 (1964) 315–320
15. Hiromi, K.; Hamauzu, Z.; Takahashi, K.; Ono, S.: Kinetic studies on gluc-amylase. II. Competition between two types of substrate having α-1,4 and α-1,6 glucosidic linkage. J. Biochem. 59 (1966) 411–418
16. Hiromi, K.; Takahashi, K.; Hamauzu, Z.; Ono, S.: Kinetic studies on gluc-amylase. III. The influence of pH on the rates of hydrolysis of maltose and panose. J. Biochem. 59 (1966) 469–475
17. Hiromi, K.; Kawai, M.; Ono, S.: Kinetic studies on gluc-amylase. IV. Hydrolysis of isomaltose. J. Biochem. 59 (1966) 476–480
18. Abduliah, M.; Fleming, I. D.; Taylor, P. M.; Whelan, W. J.: Substrate specificity of the amyloglucosidase of Aspergillus niger. Biochem. J. 89 (1963) 359–369
19. Kuo, S. S.: In: Computer applications of numerical methods. Massachusetts: Addison-Wesley Publishing Company, Inc. 1972
20. Levenspiel, O.: The Monod equation: A revisity and a generalization to product inhibition situations. Biotechnol. Bioeng. 22 (1980) 1671–1687
21. Ghose, T. K.; Tyagi, R. D.: Rapid ethanol fermentation of cellulose hydrolysate. II. Product and substrate inhibition and optimization of fermentor design. Biotechnol. Bioeng. 21 (1979) 1401–1420
22. Bazua, C. D.; Wilke, C. R. P.: Ethanol effects on the kinetics of a continuous fermentation with Saccharomyces cerevisiae. Biotechnol. Bioeng. Symp. No. 7 (1977) 105–118
23. Leudeking, R.; Piret, E. L.: A kinetic study of the lactic acid fermentation: Batch process at controlled pH. J. Biochem. Microbiol. Technol. Eng. 1 (1959) 393–412
24. Rogers, P. L.; Lee, K. J.; Tribe, D. E.: Kinetics of alcohol production by Zymomonas mobilis at high sugar concentrations. Biotechnol. Lett. 1 (1979) 165–170
25. Tan, K.: Sago production in southwest peninsular Malaysia. In: Stanton, W. R.; Flach, M. (Eds.): Proceedings of the Second International Sago Symposium, pp. 56–83. The Hague/Boston/London: Martinus Nijhoff Publishers 1980
26. Rhee, S. K.; Lee, G. M.; Han, Y. T.; Zainal, A.; Han, M. H.; Lee, K. J.: Ethanol production from cassava and sago starch using Zymomonas mobilis. Biotechnol. Lett. 6 (1984) 615–620
27. Novo Industri Enzyme Information. File Number A5170-GB (1972)
28. Lee, K. J.; Rogers, P. L.: The fermentation kinetics of ethanol production by Zymomonas mobilis. Chem. Eng. J. 27 (1983) 831–838
29. Hyung, S. Y.; Chen, J. C.: Analysis of the kinetics of ethanol fermentation with Zymomonas mobilis considering temperature effect. Enzyme Microb. Technol. 10 (1988) 431–439
30. Jobses, I. M. L.; Roels, J. A.: The inhibition of the maximum specific growth and fermentation rate of Zymomonas mobilis by ethanol. Biotechnol. Bioeng. 28 (1986) 554–563
31. Jobses, I. M. L.; Egberts, G. T. C.; Luyben, K. C. A. M.; Roels, J. A.: Fermentation kinetics of Zymomonas mobilis at high ethanol concentrations: Oscillations in continuous cultures. Biotechnol. Bioeng. 28 (1986) 868–877

Received June 18, 1991

C.-G. Lee
Department of Chemical Engineering
University of Michigan
Ann Arbor, Michigan 48109-2136
USA

C. H. Kim
S. K. Rhee (corresponding author)
Laboratory of Metabolic Engineering
Genetic Engineering Research Institute
Korea Institute of Science and Technology
P.O. Box 17
Taedok Science Town
Taejon, 305–606
Korea